Heterodimers

DOI: 10.1002/ange.201007270

Quantum Dot–Bridge–Fullerene Heterodimers with Controlled Photoinduced Electron Transfer**

*Zhihua Xu and Mircea Cotlet**

Molecular electronics has been growing rapidly, to a point where the ambition is to miniaturize conventional electronic devices down to the single-molecule scale.[1] One of the essential components of the future molecular circuits is miniaturized power sources. A few reports have addressed this key issue by using a single nanowire as a low-power source for nanoelectronics, such as a piezoelectric nanogenerator based on zinc oxide nanowire[2] and a solar cell made from a single coaxial silicon nanowire.[3] Organic donor–bridge–acceptor (DBA) supramolecules have been at the center of research interest in molecular electronics owing to their rich charge-transport mechanisms[4] and the ability to control the rate of charge transfer through chemical synthesis.[5] DBA systems can be promising power sources for molecular circuits if they efficiently absorb and convert photons into charge carriers through photoinduced charge transfer (CT). Recently, semiconductor quantum dots (QDs) have been combined with dyes, fullerenes, TiO_2, or conductive polymers to yield donor–acceptor (DA) charge-transfer systems for dye-sensitized cells or hybrid solar cells.[6] However, the power conversion efficiency of such QD-based devices remains quite low. Tremendous efforts have been devoted to unveiling the fundamentals of photovoltaic processes such as charge separation and recombination in QD-based devices, mainly by ensemble-averaged optical methods such as ultrafast transient photoluminescence and absorption spectroscopy. Recent reports demonstrate that single-molecule spectroscopy (SMS) is a powerful method to unveil the inhomogeneous dynamics of CT obscured by ensemble averaging in a variety of systems, including organic DBA systems, dyes adsorbed on TiO_2, or proteins.[7] A limited number of SMS studies addresses charge transfer between QDs and acceptor materials such as TiO_2 or an ensemble of dyes adsorbed on a QD.[8]

Herein we introduce a method to fabricate electron-transfer DBA heterodimers based on a core/shell CdSe/ZnS QD and a fullerene derivative, the interparticle distance of which is controlled by aminoalkanethiol linkers. The fabricated QD–FMH dimers provide a model system for the single-molecule exploration of photoinduced electron transfer between QDs and electron acceptors, which is an essential process in QD-based solar cells. By varying the linker length and the QD size, we demonstrate control of the rate and of the magnitude of fluctuations of the photoinduced electron transfer at the level of the individual dimers. With excellent, size-dependent light absorption properties conferred by the incorporated QDs, these dimers are promising power-generating units for molecular electronics.

The components used for fabricating the DBA heterodimers consist of a water-soluble fullerene derivative (fullerene–malonic acid hexaadduct, FMH); a set of water-soluble carboxy-ended core/shell CdSe/ZnS QDs with varying sizes and colors: QD605, QD565, and QD525, denoting QDs with photoluminescence (PL) emission maxima at 605, 565, and 525 nm, respectively; and a set of aminoalkanethiol linkers (Figure 1a). The electronic spectra of FMH and QDs are shown in Figure 1b. Owing to the lack of overlap between the PL spectra of QDs and the absorption spectrum of FMH, energy transfer from QDs to FMH is ruled out. Therefore, charge transfer from QDs to FMH should be the primary photoinduced interaction under optical excitation at 460 nm. This interaction can be further narrowed down to electron transfer (ET), considering the positioning of the electronic energy levels of CdSe QDs (conduction band −4.3 eV, valence band −6.4 eV for a 4.4 nm CdSe QD)[9] and fullerene (lowest unoccupied molecular orbital (LUMO) −4.7 eV, highest occupied molecular orbital (HOMO) −6.8 eV), which does not favor hole transfer.[10]

When QDs and FMH are mixed in aqueous solution, quenching of QDs by FMH is low (15%, see Figure S1a in the Supporting Information), presumably owing to the weak electronic coupling between QDs and FMH, as both have negatively charged carboxy groups at the surface. To enhance the electronic coupling, aminoalkanethiol linkers of varying length (Figure 1a) were used to conjugate QD and FMH components: 6-amino-1-hexanethiol hydrochloride (6AHT), 11-amino-1-undecanethiol hydrochloride (11AUT), and 16-amino-1-hexadecanethiol hydrochloride (16AHT). Specifically, the amine end of the linker couples with a carboxy group of the FMH through a standard coupling reaction assisted by 1-ethyl-3-(3-dimethylaminopropyl)carbodiimide (EDC), while the thiolated end of the linker binds to the ZnS surface of the core/shell QD.[11] This procedure enhances quenching of the QD by FMH in solution (up to 42% and for the shortest linker, see Figure S1b in the Supporting Information), thus indicating enhanced ET and therefore successful linking of QDs and FMHs by aminoalkanethiols. Enhanced ET was further confirmed by transient PL and absorption measurements in solution (see Figures S2 and S3

[*] Dr. Z. Xu, Dr. M. Cotlet
Center for Functional Nanomaterials
Brookhaven National Laboratory, Upton, NY 11973 (USA)
E-mail: cotlet@bnl.gov

[**] This research was carried out under the Office of Science US-DOE Contract No. DE-AC02-98CH10886. We thank Dr. H. L. Wang from LANL for providing the fullerene and Dr. M. Sfeir from BNL for help with transient absorption measurements.

Supporting information for this article is available on the WWW under http://dx.doi.org/10.1002/anie.201007270.

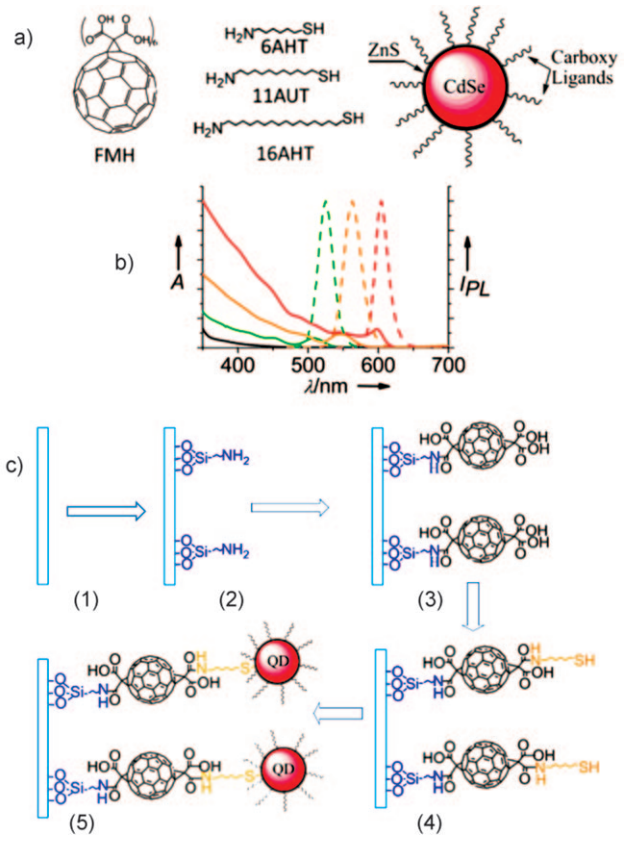

Figure 1. a) Structures of FMH, CdSe/ZnS QD, and aminoalkanethiols linkers. b) UV/Vis spectrum of FMH (black) and UV/Vis (solid lines) and PL spectra (dashed lines) of QD525 (green), QD565 (orange), and QD605 (red). *A* is absorbance, I_{PL} is photoluminescence intensity. c) Stepwise surface-based assembly of QD–FMH dimers. Steps 1–5 are described in the Experimental Section. Drawing of QDs and FMH is not to scale.

(ca. 1 nm), binding of multiple QDs to a single immobilized FMH is excluded owing to steric repulsion in this surface configuration. Conversely, by controlling the surface coverage of FMHs, we ensure that a single QD couples to only one immobilized FMH. Control experiments indicated that non-specific binding of QDs to surface-immobilized FMH molecules is negligible in the absence of aminoalkanethiols linkers (see Figure S4 in the Supporting Information).

Representative PL intensity and lifetime trajectories of an isolated QD605 particle and of single QD605–16AHT–FMH, QD605–11AUT–FMH, and QD605–6AHT–FMH dimers are shown in Figure 2. The PL intensity trajectory of a QD605

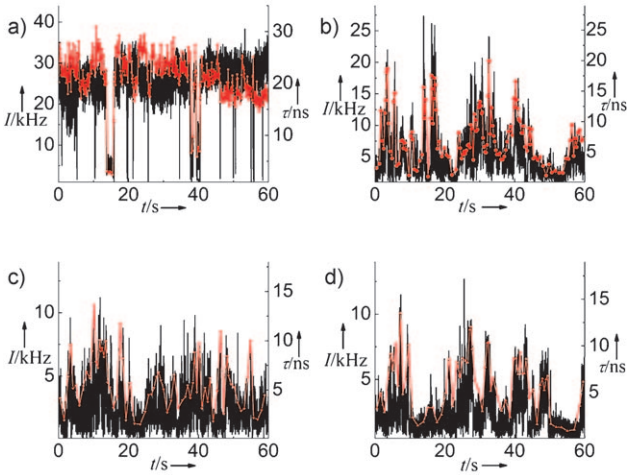

Figure 2. Single-molecule trajectories of the PL intensity (black) and lifetime (red) measured from a) QD605 and from dimers b) QD605–16AHT–FMH, c) QD605–11AUT–FMH, and d) QD605–6AHT–FMH.

in the Supporting Information). We note that control experiments showed negligible quenching of the PL of QDs by EDC and aminoalkanethiols. However, a limited yield of the EDC coupling reaction and the unavoidable cross-linking between QDs and FMH in solution results in the coexistence of isolated QD particles, dimers, trimers, and even larger structures, thus making QD–FMH conjugates highly heterogeneous. To circumvent this heterogeneity, we designed a stepwise surface-based assembly procedure that yields QD–FMH dimers of high purity (see Figure 1c and the Experimental Section). The surface assembly starts with vacuum deposition of low-molecular amine-ended silane (3-aminopropyltrimethoxysilane) on cover glass; the density of amine groups at the surface is controlled by the deposition time. Next, FMH is immobilized on the surface through EDC coupling between the amine groups on the glass surface and carboxy groups of FMH. A second EDC coupling reaction connects the aminoalkanethiol linker to the immobilized FMH, specifically the amine group of the linker and an available carboxy group in FMH. In a final step, carboxy-ended CdSe/ZnS QDs are coupled to the immobilized and thiolated FMHs. Since the size of a functionalized core/shell CdSe/ZnS QD (8–12 nm) is larger than that of FMH nanoparticle shows the typical "on–off" blinking, a signature for the presence of a single emitting nanocrystal (Figure 2a). PL intensity and lifetime values from such isolated QDs are correlated; for example, high intensity levels exhibit long lifetimes.[12] The PL intensity and lifetime trajectories of QD–FMH dimers show correlated fluctuations (Figure 2b–d), but the corresponding PL intensity and lifetime values are suppressed when compared to that of QD605, thus suggesting enhanced nonradiative recombination owing to photoinduced electron transfer from QD to FMH. Compared to the isolated QDs, the dimers exhibit different blinking dynamics, with a continuous distribution of the PL intensity, suggesting inhomogeneous electron transfer between QD and FMH.

To better demonstrate the inhomogeneity of ET in QD–FMH dimers, PL lifetime histograms were constructed from lifetime trajectories measured from 50 individual QD605 (Figure 3a) and from 50 individual QD605–FMH dimers of a given linker length (Figure 3b–d). For QD605 , the lifetimes distribute symmetrically around 20 ns (standard deviation, $\sigma \approx 6.5$ ns). For QD605–FMH dimers, the lifetime histograms are asymmetric, and peak values diminished to 5 ns ($\sigma \approx 6.7$ ns) for QD605–16AHT–FMH, 3 ns ($\sigma \approx 5.9$ ns) for QD605–11AUT–FMH, and 1 ns ($\sigma \approx 4.4$ ns) for QD605–

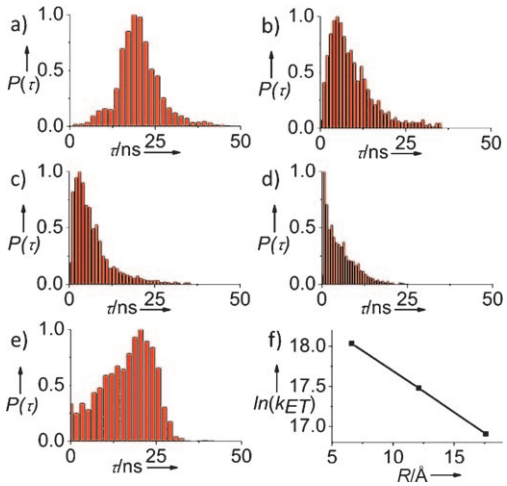

Figure 3. Histograms of single-molecule PL lifetimes, each constructed from 50 individual trajectories measured from a) QD605 nanoparticles; from dimers b) QD605–16AHT–FMH, c) QD605–11AUT–FMH, and d) QD605–6AHT–FMH; and from e) QD605 nanoparticles spincoated on an FMH film. f) Electron-transfer rate k_{ET} versus linker length R for QD605–FMH dimers.

6AHT–FMH, thus indicating an enhanced ET rate and suppressed ET fluctuation for shorter linkers. As a comparison, a PL lifetime histogram constructed from 50 individual QDs spincoated on top of a FMH thin film is shown in Figure 3e, featuring a peak at 20 ns ($\sigma \sim 7.6$ ns). This particular histogram is broader than those corresponding to QD–FMH dimers (Figure 3b–d) but is rather similar to that observed for QDs coated on TiO_2 film.[8b] This result suggests that the dimer structure significantly reduces the magnitude of fluctuations of ET between QD and FMH. The inhomogeneity of electron transfer in QD–FMH dimers leads to a distribution of PL lifetimes and ET rates. To quantify the linker-length effect on electron-transfer rate, we calculated the intensity-weighted average PL lifetime τ_{av} and the ET rate k_{ET} for QD–FMH dimers from the lifetime histograms from Figure 3b–d (see details in the Supporting Information). We found that the average ET rate exhibits an exponential dependence on linker length (Figure 3f) with an attenuation coefficient $\beta \approx 0.1$ Å^{-1}, calculated from $\ln k_{ET} = \ln k_0 - \beta R$, with linker length R. For organic DBA systems with flexible alkane bridges, bulk measurements in solution yield $\beta \approx 0.8$ Å^{-1}.[13] For QD–FMH dimers, a small value of β may point towards a complex charge-transfer mechanism.

The electron transfer is influenced not only by the D–A electronic coupling but also by the driving force (energy-band offset) between D and A moieties. The unique size-dependent energy band gap of QDs provides another effective way to control single-molecule ET in QD–FMH dimers. By decreasing the QD core size from 4.4 to 2.5 nm, the conduction band is expected to be upshifted by around 0.2 eV,[9] thus resulting in an increase of the ET driving force. PL lifetime histograms, each constructed from trajectories corresponding to 50 individual QDs and 50 individual QD–16AHT–FMH dimers with QDs of different colors (sizes), namely QD605 (core size 4.5 nm), QD565 (3.2 nm), and QD525 (2.5 nm), are shown in Figure 4a–c. Figure 4d shows the average ET rate versus QD core size calculated on the basis of the histograms from Figure 4a–c. The ET rate increases from 2.2×10^7 s^{-1} for

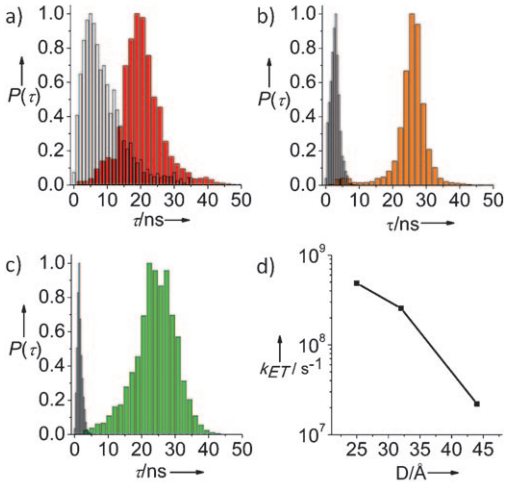

Figure 4. Histograms of single-molecule PL lifetimes each constructed from 50 individual trajectories measured from QDs and QD–FMH dimers using QDs of different sizes: a) QD605 (red) and QD605–16AHT–FMH dimer (black); b) QD565 (orange) and QD565–16AHT–FMH dimer (black); c) QD525 (green) and QD525–16AHT–FMH dimer (black). d) Electron-transfer rate versus QD size for QD–16AHT–FMH dimers.

QD605–16AHT–FMH to 4.9×10^8 s^{-1} for QD525–16AHT–FMH, consistent with the size-dependent ET observed from CdSe QDs to TiO_2.[14] One interesting phenomenon associated with the size-dependent ET rate is that ET fluctuations are suppressed in dimers with smaller QD sizes. The standard deviation of the PL lifetime is 6.7 ns for QD605–16AHT–FMH, 1.4 ns for QD565–16AHT–FMH, and 0.8 ns for QD525–16AHT–FMH. This suppression of ET fluctuation in dimers with smaller QD sizes leads to a stable charge generation rate, which can have a positive impact on the application of these dimers in molecular electronics.

To unravel the time scale of ET fluctuations in QD–FMH dimers, we used a photon-by-photon analysis method capable of probing single-molecule lifetime dynamics (fluctuations) over many orders of magnitude, from microseconds to seconds.[7a,15] The method computes autocorrelations of PL lifetimes (ACPLs) for measured single molecules on a photon-by-photon basis (see details in the Supporting Information). Typical ACPLs for a single QD and for a QD–FMH dimer are shown in Figure 5a,b. They can be roughly described by single and biexponential decay models, respectively. Fluctuations in the PL lifetime of individual QDs have been previously explained by invoking a dynamic distribution of the charge trap state.[12b,16] The variation in the trap state not only leads to fluctuations in the nonradiative recombination rate but also to variations in the QD's electronic states, as manifested by spectral diffusion,[17] a phenomenon that could influence the electron transfer to FMH. Therefore, the long time decay (over 10 ms) of the ACPLs of the QD and QD–

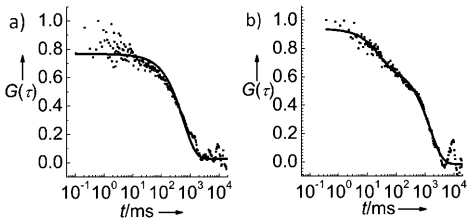

Figure 5. Photon-by-photon autocorrelations of PL lifetimes measured from a) individual QD605 and b) an individual QD605–16AHT–FMH dimer. Solid lines are single exponential ((a), 572 ms) and biexponential ((b), 25, 1490 ms) decay fits.

FMH dimer can be attributed to fluctuations of the charge-trapping state in QDs, consistent with recent findings that spectral diffusion dynamics of single QDs is slower than 10 ms.[18] In this assumption, the suppression of ET fluctuations in dimers with smaller QD sizes is understandable, because these dimers have a larger ET driving force and hence will be less prone to small fluctuations of the electronic states of the QD. Compared to a QD, the ACPLs of QD–FMH dimers exhibit a significant decay before 10 ms. These fast ET fluctuations might be due to complicated thermally induced molecular motions, similar to the situation reported for organic DBA systems.[13,19] We observed that reducing linker length in the dimer results in suppression of ET fluctuations, which indicates that linker motion plays an important role for defining and controlling the magnitude of ET fluctuation.

In summary, a series of QD–FMH dimers have been fabricated by stepwise surface assembly, and photoinduced ET in these dimers has been investigated by single-molecule spectroscopy. SMS not only reveals the linker length and QD size effect on average ET rate but also unveils the static and dynamic inhomogeneity of ET, which cannot be probed by ensemble-averaged measurements. Two distinct ET fluctuation regimes have been resolved and attributed to the variation of the trap state in the QDs and to molecular motions within dimers. Reducing linker length and QD size have been found to limit fluctuations of ET in these dimers. With well-controlled light absorption and ET rate, these dimers may find applications in miniature and large-area photovoltaics.

Experimental Section

Chemicals: Carboxy-ended core/shell CdSe/ZnS QDs (QD ITK) emitting at 605 (QD605), 565 (QD565), and 525 nm (QD525) were obtained from Invitrogen. Fullerene–malonic acid hexaadduct (FMH) was synthesized according to the published procedure.[20] Aminoalkanethiols 16-amino-1-hexadecanethiol hydrochloride, 11-amino-1-undecanethiol hydrochloride, and 6-amino-1-hexanethiol hydrochloride were obtained from Dojindo; 1-ethyl-3-(3-dimethylaminopropyl)carbodiimide hydrochloride (EDC) and 3-aminopropyltrimethoxysilane (APTMS) were obtained from Sigma Aldrich.

Dimer fabrication: The stepwise surface assembly of QD–FMH dimers included five steps (Figure 1c): 1) coverglass cleaning, 2) surface silanization, 3) FMH coupling, 4) linker coupling, and 5) QD conjugation. In brief, coverglasses were cleaned by soaking in piranha solution (30% (v/v) hydrogen peroxide, 70% (v/v) sulfuric acid) for 15 min and then thoroughly rinsed with deionized water. After drying with nitrogen gas, coverglasses were placed in a dessicator together with 20 μL APTMS under vacuum (20 kPa) for 15–120 min with subsequent heat treatment (90 °C) for one hour.[21] The amine-modified coverglasses were then covered by 100 μL mixed aqueous solution of the FMH (0.04 mg mL^{-1}) and EDC (5 mg mL^{-1}) and incubated for 30 min. The surface of the glass slides was further treated by 100 μL mixed aqueous solutions of EDC (5 mg mL^{-1}) and different aminoalkanethiols (0.01 mg mL^{-1}) for 30 min. In a final step, the glass surface was treated with diluted QD solution (0.5 nM) for 1 min. Following each of the last three steps, the coverglasses were thoroughly rinsed with deionized water to remove excess chemicals.

Characterization: SMS was performed on a home-built confocal scanning-stage fluorescence microscope (Olympus IX81) coupled with a laser system delivering 460 nm pulses at 8 MHz repetition rate (frequency-doubled, pulsed-picked Ti:Sapphire laser, Tsunami Spectra-Physics). The laser beam was then reflected by a dichroic mirror (Di01-R442, Semrock) and focused on the sample by a 100×, 1.4 NA oil objective lens (Olympus). Fluorescence was collected by the same objective lens, filtered from excitation by the dichroic mirror and a band-pass filter (FF01-583/120, Semrock), spatially filtered by a 75 μm pinhole, and focused on a single-photon-counting avalanche photodiode (APD). The signal from the APD was measured by a time analyzer (PicoHarp 300, PicoQuant). PL intensity and lifetime trajectories were recorded using the time-tagged time-resolved mode, each trajectory for 60 seconds. Lifetimes were calculated from decays of 1000 total photons by the maximum likelihood estimation method.[7b]

Received: November 18, 2010
Published online: May 5, 2011

Keywords: electron transfer · fullerenes · heterodimers · quantum dots · single-molecule studies

[1] a) J. R. Heath, M. A. Ratner, *Phys. Today* **2003**, *56*, 43; b) R. L. McCreery, A. J. Bergren, *Adv. Mater.* **2009**, *21*, 4303.
[2] Z. L. Wang, J. H. Song, *Science* **2006**, *312*, 242.
[3] B. Z. Tian, X. L. Zheng, T. J. Kempa, Y. Fang, N. F. Yu, G. H. Yu, J. L. Huang, C. M. Lieber, *Nature* **2007**, *449*, 885.
[4] a) A. Aviram, M. A. Ratner, *Chem. Phys. Lett.* **1974**, *29*, 277; b) R. M. Metzger, B. Chen, U. Hopfner, M. V. Lakshmikantham, D. Vuillaume, T. Kawai, X. L. Wu, H. Tachibana, T. V. Hughes, H. Sakurai, J. W. Baldwin, C. Hosch, M. P. Cava, L. Brehmer, G. J. Ashwell, *J. Am. Chem. Soc.* **1997**, *119*, 10455.
[5] J. Kroon, J. W. Verhoeven, M. N. Paddonrow, A. M. Oliver, *Angew. Chem.* **1991**, *103*, 1398; *Angew. Chem. Int. Ed. Engl.* **1991**, *30*, 1358.
[6] a) A. J. Nozik, *Phys. E* **2002**, *14*, 115; b) W. U. Huynh, J. J. Dittmer, A. P. Alivisatos, *Science* **2002**, *295*, 2425; c) P. Brown, P. V. Kamat, *J. Am. Chem. Soc.* **2008**, *130*, 8890.
[7] a) H. Yang, G. B. Luo, P. Karnchanaphanurach, T. M. Louie, I. Rech, S. Cova, L. Y. Xun, X. S. Xie, *Science* **2003**, *302*, 262; b) M. Cotlet, S. Masuo, G. B. Luo, J. Hofkens, M. Van der Auweraer, J. Verhoeven, K. Mullen, X. L. S. Xie, F. De Schryver, *Proc. Natl. Acad. Sci. USA* **2004**, *101*, 14343; c) Y. M. Wang, X. F. Wang, S. K. Ghosh, H. P. Lu, *J. Am. Chem. Soc.* **2009**, *131*, 1479; d) L. J. Guo, Y. M. Wang, H. P. Lu, *J. Am. Chem. Soc.* **2010**, *132*, 1999; e) M. Sauer, *Angew. Chem.* **2003**, *115*, 1834; *Angew. Chem. Int. Ed.* **2003**, *42*, 1790; f) M. W. Holman, R. C. Liu, L. Zang, P. Yan, S. A. DiBenedetto, R. D. Bowers, D. M. Adams, *J. Am. Chem. Soc.* **2004**, *126*, 16126.
[8] a) J. Huang, D. Stockwell, Z. Q. Huang, D. L. Mohler, T. Q. Lian, *J. Am. Chem. Soc.* **2008**, *130*, 5632; b) S. Y. Jin, T. Q. Lian, *Nano Lett.* **2009**, *9*, 2448; c) S. C. Cui, T. Tachikawa, M. Fujitsuka, T. Majima, *J. Phys. Chem. C* **2008**, *112*, 19625.

[9] N. C. Greenham, X. G. Peng, A. P. Alivisatos, *Phys. Rev. B* **1996**, *54*, 17628.
[10] D. F. Liu, W. Wu, Y. F. Qiu, J. Lu, S. H. Yang, *J. Phys. Chem. C* **2007**, *111*, 17713.
[11] S. Ravindran, S. Chaudhary, B. Colburn, M. Ozkan, C. S. Ozkan, *Nano Lett.* **2003**, *3*, 447.
[12] a) X. D. Ma, H. Tan, T. Kipp, A. Mews, *Nano Lett.* **2010**, *10*, 4166; b) K. Zhang, H. Y. Chang, A. H. Fu, A. P. Alivisatos, H. Yang, *Nano Lett.* **2006**, *6*, 843.
[13] G. L. Closs, J. R. Miller, *Science* **1988**, *240*, 440.
[14] I. Robel, M. Kuno, P. V. Kamat, *J. Am. Chem. Soc.* **2007**, *129*, 4136.
[15] H. Yang, X. S. Xie, *J. Chem. Phys.* **2002**, *117*, 10965.
[16] R. Verberk, A. M. van Oijen, M. Orrit, *Phys. Rev. B* **2002**, *66*.
[17] R. G. Neuhauser, K. T. Shimizu, W. K. Woo, S. A. Empedocles, M. G. Bawendi, *Phys. Rev. Lett.* **2000**, *85*, 3301.
[18] L. F. Marshall, J. A. Cui, X. Brokmann, M. G. Bawendi, *Phys. Rev. Lett.* **2010**, *105*, 053005.
[19] W. B. Davis, M. A. Ratner, M. R. Wasielewski, *J. Am. Chem. Soc.* **2001**, *123*, 7877.
[20] I. Lamparth, A. Hirsch, *J. Chem. Soc. Chem. Commun.* **1994**, 1727.
[21] A. S. Anderson, A. M. Dattelbaum, G. A. Montano, D. N. Price, J. G. Schmidt, J. S. Martinez, W. K. Grace, K. M. Grace, B. I. Swanson, *Langmuir* **2008**, *24*, 2240.

